Architecture of bacterial respiratory chains

Ville R. I. Kaila[1†] and Mårten Wikström[2]

[1]Department of Biochemistry and Biophysics, Stockholm University, Stockholm, Sweden. [2]Institute of Biotechnology, University of Helsinki, Helsinki, Finland.

[†]**E-mail:** ville.kaila@dbb.su.se

Abstract: Bacteria power their energy metabolism using membrane-bound respiratory enzymes that capture chemical energy and transduce it by pumping protons or Na^+ ions across their cell membranes. Recent breakthroughs in molecular bioenergetics have elucidated the architecture and function of many bacterial respiratory enzymes, although key mechanistic principles remain debated. In this Review, we present an overview of the structure, function, and bioenergetic principles of modular bacterial respiratory chains and discuss their differences to the eukaryotic counterparts. We also discuss bacterial supercomplexes, which provide central energy transduction systems in several bacteria, including important pathogens, and which could open up possible avenues for treatment of disease.

Introduction

Bacteria have a fascinating energy metabolism, which enables them to survive in a wide variety of harsh surroundings, from acidic ponds and hot springs to anaerobic intestines of animals. Their remarkable ability to adapt to their environment is reflected on the molecular level by the function of modular respiratory chains, consisting of the enzyme complexes I, III, and IV, which catalyse the bacterial energy conversion process. These complexes catalyse the oxidation of NADH (produced by oxidation of nutrients) by quinone, oxidation of the quinol by cytochrome *c*, and oxidation of cytochrome *c* by O_2, respectively. Under aerobic conditions these membrane-bound energy transducers extract 'high-energy' electrons from a wide variety of chemical substrates, depending on the growth conditions, transfer them to dioxygen, which is reduced to water, and convert the free energy of the process to a proton or a sodium motive force (PMF or SMF) by translocating protons or sodium ions across the cell membrane[1]. Under anaerobic conditions other ultimate electron acceptors may be used, such as nitrite and nitrate, or even molecules such as dimethylsufoxide (DMSO). The ion motive force normally operates around 100-180 mV[2], and drives synthesis of adenosine triphosphate (ATP) from adenosine diphosphate (ADP) and inorganic phosphate (P_i)[3]. The PMF also drives active transport of solutes against their concentration gradient by secondary active transporter proteins[1], which also link the Na^+ and H^+ energetics together[4]. The established PMF consists of both electrical ($\Delta\psi^{out\text{-}in}$) and pH gradients ($\Delta pH^{out\text{-}in}$), which give rise to the chemiosmotic force across the membrane[1]. In bacteria that grow at neutral pH (for example, *E. coli*), the PMF is mainly composed of the electrical membrane potential, as in mitochondria, whereas in several

pathogens, such as *Helicobacter pylori* and *Salmonella enterica*, the ΔpH component[5] between an acidic outside and an alkaline cytoplasm is dominating.

The core physical principles of respiratory chains are strongly conserved across all domains of life. However, in stark contrast to linear electron transport chains of eukaryotic mitochondria, bacteria have branched respiratory chains, which can use different routes of electron transfer depending on the growth conditions, for example, for oxidising the quinol by O_2 either via *c*-type cytochromes or directly. In contrast to eukaryotes, certain bacteria can also switch between aerobic and anaerobic conditions (the facultative anaerobes), in which, for example, formate is oxidised by fumarate or nitrate instead of dioxygen[6,7]. Due to a large variation between bacterial respiratory chains, only a few selected examples are shown in Fig. 1, with focus on the aerobic soil-bacterium *Paracoccus denitrificans*, comprising a branch that in many parts resembles mitochondrial respiration, and that of *Escherichia coli*, which is a central model organism in microbiology, but has a rather exotic energy metabolism (Fig. 1). The main focus of this Review is on aerobic respiratory chains of bacteria with only a limited number of examples from the archaeal world.

The exact molecular principles of all bacterial, archaeal, and indeed mitochondrial energy-transducing enzymes are still not fully understood, but they are all structurally and functionally related to each other. The field underwent a giant leap in the recent decade by resolved molecular structures due to advances in both membrane protein crystallography and cryo-electron microscopy (cryo-EM) (Table 1). This structural data has provided a blueprint for further functional and mechanistic studies by various approaches[8]. In this Review, we present an overview of key bioenergetic and structural aspects of the main respiratory enzyme complexes I, III, and IV that have been resolved in recent years, and the implications for understanding the molecular principles of bacterial energy transduction.

Bioenergetic principles

Bacterial respiratory chains have redox spans of > 1 Volt, which are established between electron-donating carriers such as nicotinamide adenine dinucleotide ($NADH/NAD^+$, $E_{m,7}$=-320 mV; redox midpoint potential at pH=7 relative to the normal hydrogen electrode (NHE)), flavin adenine dinucleotide ($FADH_2/FAD$, $E_{m,7}$=+31mV), formate (HCO_2^-/CO_2 $E_{m,7}$=-420 mV), succinate (succinate/fumarate, $E_{m,7}$=+31 mV) and hydrogen (H_2/H^+, $E_{m,7}$=0 mV), and small inorganic electron acceptors with high electron affinities, the most prominent ones being O_2/H_2O ($E_{m,7}$=+815 mV) and NO/N_2O ($E_{m,7}$=+1300 mV). This redox span gives rise to a thermodynamic driving force of > 1 eV (around 23 kcal mol^{-1} or 96 kJ mol^{-1}, $\Delta G=-nF\Delta E_m$ with

n being the number of electrons and *F* the Faraday's constant (~96,485 C mol^{-1})), which is conserved by pumping protons or Na^+ ions across the bacterial membrane. On a more detailed chemical level, the respiratory enzymes catalyse proton-coupled electron transfer (PCET) reactions, in which the motion of the two elementary particles is tightly linked. With a high PMF of around 200 mV, each proton transport across the membrane has a thermodynamic cost of around 4.6 kcal mol^{-1} (19.2 kJ mol^{-1}), and thus with a ~1 V redox span between the initial donor and acceptor (for example, NADH and O_2), up to 5 H^+ are pumped for each transferred electron. The stepwise drop in potential along the respiratory chain enables the redox energy to be conserved rather than dissipated as heat, and the respiratory enzymes to operate at a high thermodynamic efficiency.

Several bacteria can also power their energy conversion using a SMF (Δp_{Na^+}), which is established by the sodium-translocating NADH:ubiquinone oxidoreductase (Nqr, Fig. 2, see below) or oxaloacetate decarboxylase (oadGAB)[9], and switch between H^+ and Na^+ pumping modes[4] through the Na^+/H^+ antiporters[10]. For a review on bacterial Na^+ energetics, the reader is referred to Ref.[11]

The lipid membrane also forms an integral part of the protonmotive respiratory machinery. In addition to providing an isolating layer that stores the PMF, the lipid headgroups have been suggested to establish proton conduction pathways along the membrane surface[12], and to participate in proton uptake in respiratory complexes[13], although exact mechanistic principles of lipid-mediated proton conduction is still not fully understood[14, 15]. The lipids may also have functional roles in stabilising respiratory supercomplexes, that is, assemblies of the individual enzyme complexes, possibly regulating their activity (see below)[16, 17]. Overall, the bacterial membranes have a diverse lipid composition[18], but many of them are composed of zwitterionic lipids **[G]** such as phosphatidylethanolamine (75% in *E. coli*), and anionic lipids such as phosphatidylglycerol (20% in *E. coli*) and cardiolipin (5% in. *E. coli*). Moreover, the cytoplasmic membrane of, for example, actionbacteria comprises highly glycosylated lipids with phosphatidylinositol and phosphatidylinositol mannoside, which affect the physicochemical properties of the membrane. Interestingly, phosphatidylcholin, which forms 40% of the inner mitochondrial membrane, occurs less commonly in bacteria[18].

Proton conduction channels within the respiratory enzymes[8, 19] are used to overcome the high desolvation (Born) free energy **[G]** of transferring protons or ions across the low dielectric of the membrane. On the molecular level this is achieved by water molecules[20] and protonatable protein residues (for example, Tyr, Glu, Asp, His, Ser, and Thr)[21], which establish 'proton wires' , and enable the charge rather than the proton itself to be transferred in a Grotthuss-type

hopping process **[G]**[20]. To achieve active proton pumping, the respiratory enzymes convert the free energy of the redox reactions to pK_a-modulation in buried titratable groups within the proton channels. In contrast to protons that require conduction channels, electrons are nearly 2000-times smaller elementary particles, and their motion is governed by quantum mechanical principles[22-26]. Most redox reactions are catalysed by metal centres embedded within in the respiratory enzymes, and enable electron transfer by quantum mechanical tunnelling. The rate of these electron transfer processes is determined by the thermodynamic driving force set by the redox potential difference between the donor and acceptor groups, the reorganisation energy associated with the structural relaxation upon oxidoreduction, as well as by the degree of electronic coupling between the donor and acceptor, which depends on the distance between the two[22-24]. Many redox active centres in the respiratory complexes comprise iron-sulphur (FeS) clusters, flavine, quinone and heme groups that are relatively close in redox potential, have modest reorganization energies of 0.2-0.7 eV, and are positioned within a 5-14 Å edge-to-edge separation to enable charge separation on biologically relevant nanosecond to millisecond time scales[24-26].

Bacterial cell respiration is a non-equilibrium process, in which the efficiency is determined by the charge flux (charge transferred per time unit) and the thermodynamic driving force[27]. The free energy that is not conserved in proton pumping, synthesis of ATP, or active transport, dissipates as heat. The bioenergetic cost associated with synthesis of an ATP molecule is determined by the [ATP]/[ADP][P_i] ratio, the so-called phosphorylation potential, and the standard free energy of ATP synthesis. Under 'typical' microbial conditions ΔG is ~11 kcal mol^{-1} (48 kJ mol^{-1}) in *E. coli*[28].

Due to the unique pseudo-symmetric architecture of the catalytic F_1-domain of F_oF_1-ATP synthase, formation of each ATP requires translocation of $n/3$ protons, where n is the number of subunits in the membranous *c*-ring of the F_o-part[29]. The F_oF_1-ATP synthase of *E. coli* and *P. denitrificans* have 10 and 12 *c*-rings, and the bacterial proteins therefore translocate 3.33 H^+ and 4 H^+ for the synthesis of each ATP molecule, respectively. F_oF_1-ATP synthases with 7-16 *c*-ring subunits have been discovered in recent years[29-32], suggesting that cell respiration in different organisms may run in different 'gears'. The Na^+-driven F_oF_1-ATP synthases operate by binding Na^+ to the *c*-ring, and there are some promiscuous isoforms that can operate with both Na^+ and H^+ [32]. The reader is referred to recent work on the structure and function of bacterial F_oF_1-ATP synthase in Refs.[29, 31].

The bioenergetic efficiency of oxidative phosphorylation can be characterised by the phosphate/oxygen (P/O) ratio, which determines the number of ATP molecules synthesised per

transfer of two electrons, that is, ATP/2e^-. When the P/O ratio is multiplied by the number of protons required for synthesis of one ATP molecule (H^+/ATP), one obtains the number of protons pumped per two electrons, ($H^+/2e^-$) = (ATP/2e^-) x (H^+/ATP)[33], which can be used for determining the bioenergetic efficiency under different respiratory conditions. However, although the H^+/ATP stoichiometry is quite precisely dictated by the structure of the F_oF_1-ATP synthase[34-36], determination of the P/O ratio must be approached by appropriate statistical analysis of experimental data[37]. During growth, bacterial oxidative phosphorylation operates at an overall thermodynamic efficiency of around 30%[38], which may, however, be close to optimal thermodynamic limits[39].

Overview of the molecular architecture

Electrons enter bacterial respiratory chains from two-electron carriers, such as nicotinamide and flavin adenine dinucleotide (NADH and FAD), hydrogen, or succinate, which provide electrons to complex I enzymes of type I and II, hydrogenases, and complex II, respectively. The electrons can also enter from oxidation of different organic compounds, for example, methanol through methanol dehydrogenase (PDB ID: 1H4I), methylamine through methylamine dehydrogenase (PDB ID: 2BBK) and amicyanin (PDB ID: 3C75), or formate, through formate dehydrogenase (PDB ID: 1KQF).

The initial respiratory complexes transfer the electrons to quinones, which are aromatic heterocyclic compounds that carry two electrons in the form of the reduced quinol species (QH_2). In contrast to many highly reactive and unstable free radicals, the one-electron reduced semiquinone species ($Q^{\bullet/-}$ or $QH^{\bullet}$) is relatively stable, which is of mechanistic importance for several respiratory enzymes[40]. The membrane-bound quinones have a carbon tail comprising 1-10 isoprenoid units, and an aromatic headgroup that varies between different bacteria, most notably, high potential quinones such as ubiquinone (Q, $E_{m,7}$=+90 mV), plastoquinone of photosynthetic bacteria ($E_{m,7}$=+119 mV), and caldariella quinone of thermophilic and acidophilic bacteria ($E_{m,7}$=+100 mV), as well as low potential quinones, such as menaquinone ($E_{m,7}$=-80 mV) and related species[41]. In several bacteria[41,42], the quinones can be switched between high and low potential forms depending on O_2 pressure, providing unique adaptation benefits.

In *P. denitrificans*, the membranous pool of ubiquinone is reduced not only by NADH through complex I, but also by succinate through complex II (succinate dehydrogenase, PDB ID: 1NEK [43]), yielding fumarate, a reaction that is a part of the citric acid cycle, but does not contribute to generation of PMF. The reduced Q-pool provides electrons further to complex III

(cytochrome bc_1), from where the electrons continue byt the way of the soluble electron carrier cytochrome *c* (*cyt c*, $E_{m,7=}$+250 mV) to terminal heme-copper oxidases (HCOs, or complex IV) (Fig. 1a). Depending on the growth conditions and the bacterial species, different terminal oxidases may be expressed[44]. The HCOs shuttle the electrons further to O_2, which is reduced to water, and couple the free energy to proton pumping across the bacterial membrane. In *P. denitrificans*, a central step of nitrogen metabolism is catalysed by the NOR-family of HCOs that reduce NO to N_2O (Fig. 1a, Fig. 3)[45, 46]. The respiratory branch from NDH-1 through complex III to complex IV thus closely resembles the mitochondrial respiratory chains, whereas the alternate pathways have no eukaryotic counterparts. *P. denitrificans* can also express a terminal bb_3 quinol oxidase[47], which may result in respiratory modes that resemble that of *E. coli* (see below).

Although *E. coli* is one of the most commonly used microbial model systems, the wiring of its respiratory chain differs substantially from the mitochondrial counterparts, most notably by the lack of complex III, which catalyses the oxidation of quinol by cytochrome *c* in many respiratory but also in photosynthetic electron transport chains (Fig. 1b). Electrons enter *E. coli* via NADH by both type-I and type-II complex Is (NDH-1 and NDH-2) that reduce the Q_8 pool, from where the electrons continue to the terminal bo_3-type or *bd*-type oxidases, which catalyse quinol oxidation by molecular oxygen (Fig. 1). The bo_3 oxidase pumps protons with a stoichiometry of 2 H^+/e^- [48, 49], and bd-I is also electrogenic with a stoichiometry of 1 H^+/e^- [50], although it is not a proton pump, whereas bd-II is reported to be non-electrogenic, although results differ[51, 2]. Expression of the *bd*-oxidases depends on the growth conditions[50], and is important for survival of *E. coli* under micro-aerobic conditions.

Complex I as electron entry point

Bacteria use three enzyme families as initial catalysts for electron transfer between NADH and quinone (Fig. 2)[52]. The type-I NADH:ubiquinone oxidoreductases (NDH-1) are redox-driven proton pumps that translocate 2 H^+/e^-, and are closely related to the mitochondrial complex I. Bacteria also express the unrelated non-electrogenic (0 H^+/e^-) alternate Type-II NADH:ubiquinone oxidoreductase (NDH-2)[53], and, in addition, a sodium-translocating NADH:ubiquinone oxidoreductase (Na^+-Nqr, 1 Na^+/e^-)[54, 55], which is also unrelated to the canonical complex I superfamily. *E. coli* expresses both NDH-1 and NDH-2, depending on the growth conditions[2, 44].

The canonical bacterial complex I is an L-shaped, 0.5 MDa modular enzyme complex that comprises 14 conserved core subunits that are highly homologous counterparts of the larger

45 subunit mammalian complex I[8, 56-58]. Complex I catalyses electron transfer by a chain of 8-9 FeS centres that are embedded in its hydrophilic domain, providing a tunnelling wire for the electrons between NADH and quinone[59-62]. Reduction of quinone to quinol in a binding site, located around 20 Å above the membrane plane, triggers proton pumping across the membrane domain (Fig. 2).

Complex I transduces the free energy gained from two-electron transfer between NADH and Q ($\Delta G_{NADH \rightarrow Q}$=-0.42 eV per electron), which, depending on the quinone type (see above), can be used to pump up to four protons across the bacterial membrane. A smaller pumping stoichiometry is expected when bacteria operate using lower potential quinones such as menaquinone ($\Delta G_{NADH \rightarrow MQ}$=-0.24 V per electron). The redox-driven proton pumping is fully reversible, and the enzyme can thus also drive NAD^+ reduction by quinol, powered by PMF. Such reverse electron transfer (RET) is relevant under hypoxic conditions in mitochondria[63], but it is unclear whether it is used in bacterial energy metabolism.

The membrane domain of complex I comprises antiporter-like subunits, which have evolved from bacterial multi-resistance and pH-adaptation (Mrp) transporters and which function as secondary active Na^+/H^+ transporters. The antiporter-like NuoL, NuoM, and NuoN subunits of *E. coli* complex I are responsible for pumping one proton each, whereas the fourth proton is most likely pumped via the NuoH/A/J/K subunits[8, 64]. The electron transfer domain in complex I arose from the family of NiFe-hydrogenases[65]. In exotic members of the complex I-family, the Q reduction site is replaced by a H^+ reducing NiFe-active site such as in the archeon *Pyrococcus furiosus*[66]. This family is related to membrane-bound hydrogenases that have an important role in the bioenergetics and virulence of certain bacteria[67].

In photosynthetic bacteria such as *Thermosynecoccus elongatus*, complex I has undergone modular adaptations that enable crosstalk with the photosynthetic machinery[68-71]. To this end, electrons are transferred from ferredoxin ($E_{m,7}$=-420 mV) instead of NADH, and in the NDH-1MS subfamily, the redox-coupled proton pumping machinery drives concentration of CO_2 using a unique Zn^{2+}-site within the CupA subunit[68].

Although the exact molecular mechanism of how the redox energy is converted into proton pumping up to 200 Å away from the active site of complex I still remains unclear, recent studies suggest that the long-range process involves an electrostatic wave that propagates by coupled conformational, electrostatic, and hydration changes along the membrane domain of the complex[8, 72, 73, *cf.* also 56-58, 74].

The alternate Type-II NADH:ubiquinone oxidoreductases comprise small three subunit membrane-bound enzymes that also transfer electrons from NADH to quinone (Fig. 2).

However, they are unrelated to Type I NADH:ubiquinone oxidoreductases, and belong instead to the two-dinucleotide binding domains flavoprotein-superfamily, which contains several proteins important for the bacterial metabolism. The non-electrogenic NDH-2 enzymes contribute to the respiratory chain by reducing the Q pool, but they do not generate PMF. NDH2 is bound to the membrane by amphipathic helices instead of typical transmembrane segments. A recent structure determined from *S. aureus*[75], in addition to the eukaryotic enzyme[76, 77], provides starting points for understanding their mechanism. NDH2 could be a promising drug target[5, 78] due to the lack of this protein in mammalian mitochondria.

The Na^+-translocating NADH:quinone oxidoreductases (Na^+-NQR) function as redox-driven sodium pumps (Fig. 2)[54], and are also unrelated to both NDH1 and NDH2, but instead contain subunits related to the *Rhodobacter* nitrogen fixation complex[79]. The recent structure of Na^+-NQR from *Vibrio cholerae* suggests how electron transfer from NADH through the enzyme's FAD, FeS, non-heme Fe centre, flavin and riboflavin groups, leads to the stepwise reduction of Q to QH_2 (Fig. 2)[79, 80]. The quinone reduction and electron transfer drive Na^+ pumping in the NqrB subunit, which is structurally related to urea and ammonia transporters (Fig. 2).

The redox-loop of complex III

The prokaryotic complex III or cytochrome bc_1 (ubiquinone:cytochrome *c* oxidoreducase) is a dimeric ~ 0.5 MDa membrane protein that transfers electrons between quinol and cytochrome *c* and couples the process to generation of PMF by a redox-loop process[40]. In photosynthetic bacteria, this function is achieved by the homologous cytochrome b_6f [81], which transfers electrons between plastoquinone and plastocyanin, shuttling them between photosystem II (PSII) and photosystem I (PSI). Complex III comprises a cytochrome *b* subunit with a high- and low-potential heme cofactor, heme b_H and heme b_L, as well as a Rieske iron-sulphur protein **[G]** and two Q-binding sites, located on opposite sides of the membrane. The Q_o site catalyses quinol oxidation close to the P-side (positively charged periplasmic or luminal side) of the membrane, whereas the Q_i site is connected to the N-side (negatively charged cytoplasmic or stromal side).

In contrast to complexes I and IV that pump protons across the complete membrane dielectric, complex III operates by a Mitchellian redox-loop mechanism **[G]**, in which the electrical charge moves across the membrane by transmembrane electron transfer, whereas the protons are transferred electroneutrally in the form of hydrogen (quinol)[40]. This Q-cycle mechanism[82] is initiated by QH_2 oxidation at the Q_o site, where the two electrons are transferred

by a bifurcated pathway. One of the branches lead through the Rieske FeS site to cytochrome c_1 and the soluble cytochrome *c*, whereas the second branch leads across the membrane through the b_L and b_H hemes to the Q_i site on the N-side, which is responsible for reducing a second quinone molecule (Fig. 3a, b). Oxidation of the Q_o site quinol triggers proton release to the P-side, and diffusion of the resulting oxidised quinone to the membrane pool. The reaction cycle is completed by a second QH_2 binding to the Q_o site, release of the electrons and protons as before, and reduction of the semiquinone to quinol at the Q_i site, coupled to uptake of two protons from the N-side (Fig. 3b).

Bacterial complex III can, in addition to ubiquinone, also operate with low potential quinones, such as menaquinone ($E_{m,7}$=-80 mV). On a molecular level, this has been achieved by substitutions in the highly conserved PEWYW-motif of the Q_o-site[83], and introduction of a low-potential Rieske FeS centre (+150 mV) instead of the high potential iron-sulphur protein (>+260 mV) in combination with ubiquinone[83] to level off the energetic differences, and possibly to prevent dissipation of the energy as heat.

The alternative complex III (ACIII), recently discovered in *Rhodobacter marinus*[84] and *Chloroflexus aurantiacus*[85], oxidises quinol and transfers the electrons to cytochrome oxidase, but without any structural similarity to the canonical complex III enzymes. By contrast, ACIIIs comprise 3Fe-4S and 4Fe-4S clusters and six heme cofactors, which transfer electrons to the complex IV subunit (Fig. 3c). The structure of ACIII in supercomplex with cytochrome aa_3 from *Flavobacterium johnsoniae* was recently determined[86], and provides a unique system to understand the function of bacterial supercomplexes (see below).

Modular adaptations of cytochrome *c*

The electrons of complex III are carried by the small, ~12 kDa, soluble electron carrier protein cytochrome *c* (*cyt c*) that shuttles electrons between complexes III and IV. C*yt c* has a heme C cofactor covalently linked to cysteine residues in a highly conserved CXXCH motif, but the overall architecture of the protein varies in different bacteria. *P. denitrificans* used a soluble *cyt c*, similar to that in mitochondria, but certain bacteria, such as *B. subtilis*, use both membrane, lipid and peptide anchored *cyt c*-modules[87]. Moreover, in actinobacteria the *cyt c* modules are fused either to the terminal oxidase or to the complex III protein, as revealed by the recently discovered III_2-IV_2 supercomplex from *Mycobacteria smegmatis* and *C. glutamicum* (see below)[16, 17, 88]. A similar fused *cyt c*-module can also be found in terminal oxidases, such as cytochrome cbb_3 [89] and cytochrome caa_3 [90].

Terminal respiratory oxidases

The terminal heme-copper oxidoreductases (HCOs) function as redox-driven proton pumps that used the free energy gap ($\Delta G_{cyt\ c/Q/MQ \rightarrow O2}$~-0.6 – -0.9 eV per electron) between the electron donor *cyt c* ($E_{m,7}$=+250 mV) or quinone[91]/menaquinone[92] ($E_{m,7}$=+90/-80 mV), and the electron acceptor O_2 ($E_{m,7}$=+815 mV). Electrons from *cyt c* on the periplasmic P-side of the membrane, or from quinol within the membrane, are transferred to the active site. Protons are taken up from the opposite cytoplasmic N-side of the membrane along proton conducting channels both to the active site to complete the O_2 reduction chemistry ($O_2 + 4e^- + 4H^+ \rightarrow 2H_2O$), as well as across the membrane to the periplasmic P-side (proton pumping) (Fig. 4). Interestingly, both proton pumping and the vectorial arrangement of the electron and proton transfers of the O_2 reduction chemistry contribute equally to the generation of PMF[19, 93, 94].

The HCO superfamily comprises A-, B-, and C-type members, as well as the NOR-subfamilies, which differ in their overall structural architecture, chemical composition of the embedded heme-cofactors, and electron donor groups (*cyt c* or quinone) (Fig. 4)[95]. The eukaryotic mitochondrial respiratory chains solely rely on the A-type oxidases, whereas bacteria express all three type of oxidases depending on the growth conditions. For example, *P. denitrificans* also express the NOR-family of HCOs, which is responsible for respiration by conversion of NO into N_2O[45, 46].

The A-type HCOs pump one proton across the membrane for each electron and proton transferred to the active site, thus leading to a thermodynamic stoichiometry of $2H^+/e^-$, whereas less efficient proton pumping has been reported for the B- [96] and C-type families (Fig. 4a)[97]. Although the thermodynamic driving force for the NO reduction is around 0.5 V higher than that of O_2 reduction, the *cyt c*-dependent cNOR is reported to be non-electrogenic[98], and dissipates the energy instead of using it for proton pumping for reasons that still remain unclear (Fig. 4b)[99]. Recent studies, nevertheless suggest that the quinol-oxidising qNOR is electrogenic (Fig. 1a)[100].

The terminal HCOs comprise a central conserved core subunit with an electron-queuing *a*- or *b*-type heme, and an active site composed of heme $a_3/b_3/o_3$, and a copper centre, Cu_B, at which the reduction of oxygen to water takes place. Cu_B is coordinated in all HCOs by three histidine residues, one of which forms a unique chemical crosslink to a tyrosine residue[19]. The chemical intermediates of the reaction cycle catalysed by canonical HCOs is rather well understood[19, 101], and provides a good starting point for mechanistic understanding of the more exotic bacterial HCOs.

Mechanistic studies over the last decades suggest that the inter-heme electron transfer directs protons both to the active site and across the membrane in the A-type of oxidases[19, 102-106]. Although exact details remain unclear, both electric field variations and water molecules are likely to provide central elements in the pumping mechanism by sorting protons and preventing them from leaking backwards during the pumping process[19, 102-106].

The protons are taken up by two water-filled proton transfer pathways, the D- and K-channels in the A-family, whereas the *cbb*$_3$-type oxidases of certain pathogenic proteobacteria, such as *Vibrio cholerae* and *Helicobacter pylori*, rely on only the K-channel counterpart to conduct all protons (Fig. 4a)[89, 107]. To survive under low O_2 conditions, the active site heme b_3 domain has also been modified by a carboxylate, which establishes a higher affinity for O_2 that is important in a micro-aerobic environment[89, 107]. These adaptations possibly enable the *cbb*$_3$ oxidases to reduce NO to N_2O, which is the main task of the NOR-family[109, 110], although in NORs, the Cu_B has been replaced by an Fe_B site and the conserved histidine-tyrosine of the other HCOs is also missing [45, 46].

In the *bo*$_3$ oxidases that form the terminal oxidases in *E. coli* (Fig. 4a), electrons enter directly from quinone to the electron-queuing heme *b* centre from the membrane, instead of using a *cyt c*-mediated pathway via Cu_A, and the protons released upon oxidation of QH_2 are ejected to the P-side. The *bo*$_3$:s use the chemically unusual heme O[48, 49, 109] in the oxygen reduction site, but the enzymes otherwise resemble the A-type HCOs.

In contrast to terminal proton-pumping HCOs, the structurally unrelated *bd*-type oxidases also catalyse the reduction of O_2 to H_2O by quinol, but do not pump protons[50]. The catalytic core of the recently resolved *bd*-type oxidases from *E. coli*[111] comprises three heme cofactors, and an electron queuing *b*-heme, with a high affinity O_2-reduction site formed at heme *d*, located within the dimeric CydA core of the enzyme (Fig. 4b). The electrons enter from a Q-binding loop via Q_8 in the CydB subunit that is exposed to the periplasmic side. Many pathogenic bacteria, such as the enterohemorrhagic *E. coli* and *Salmonella enterica*, use a long Q-loop domain (L variant) that could provide important drug targets, whereas some bacteria express short loop Q domains (S variant). The *bd*-oxidases also contain a single CydX subunit, which stabilises the overall *bd*-oxidase structure[111, 112], as well as a non-catalytic CydH subunit, which interacts with lipids and stabilises the oxygen channel into the active site. The *bd* oxidases are related to a class of cyanide insensitive oxidases (CIOs), named after their lack of cyanide binding, in contrast to other HCOs. The cioA/B subunits of CIOs are homologous to CydA/B of cytochrome *bd*, but the heme *d* is replaced by heme *b*[127]. These cytochrome *bb'*:s are

important for respiration in, for example, *Pseudomonas aeruginosa*, a pathogenic bacterium that can synthesize HCN.

Respiratory supercomplexes

In recent years, it has become clear that the respiratory enzymes are organised into larger supercomplexes[113] comprising different modular units of I-III_2 [114, 115], AIII-IV[86], I-III_2-IV [115], and III_2-IV_2 [16, 17, 88], with lipid molecules, in particular cardiolipin, gluing the complexes together. Most supercomplexes have so far been identified in mitochondria, but, for example, actinobacteria also use obligate respiratory supercomplexes for their energy transduction.[16, 17, 113] The function of supercomplexes is currently not well understood, but it has been suggested that they could provide a kinetic advantage[116], have a role in substrate channelling although this is in discussion[117,118], or limit non-specific contacts between different membrane-bound proteins[119], which in turn could optimise the electron flux through the respiratory chains.

The recently determined III_2IV_2 supercomplex from *M. smegmatis*[16, 17] (Fig. 5) shows modular adaptations, in which the *cyt c* has been hard-wired between complexes III and IV, and additional subunits that shield both proton channels and the contact between the electron transfer subunits. The *M. smegmagtis* III_2IV_2 supercomplex also has a unique dynamically flexible superoxide dismutase (SOD) unit that is anchored to the membrane domain of the supercomplex, and could have a functional role in shuttling electrons within the system. Interestingly, Q203, an anti-mycobacterial drug used for treatment of tuberculosis, inhibits III_2IV_2 supercomplex, possibly by blocking the Q_o-binding pockets[17]. Blocking the energy transduction or collapsing the PMF could provide possible ways to treat pathogenic bacteria as alternatives to traditional antibiotics[5]. However, most compounds that collapse the PMF (for example, valiomycin and gramicidin) or inhibit specific respiratory chain complexes (.for example, piericidin, rotenone, stigmatellin and oligomycin) also affect the eukaryotic counterparts. The unique architectures of the bacterial respiratory enzymes and their supercomplexes could therefore provide new avenues for development of drugs that specifically block the bacterial energy transduction machinery.

Concluding remarks

We have discussed the structure and function of bacterial respiratory chains, which convert the energy from redox reactions into an electrochemical proton (or sodium) gradient stored across the bacterial cytoplasmic membrane. In contrast to eukaryotes, bacteria use branched and highly

modular respiratory chains, with several electron entry sites and alternative terminal acceptors. Whereas certain bacteria, such as the soil-bacterium *P. denitrificans* have branches that closely resemble the mitochondrial respiratory chains, others, such as *E. coli,* have an atypical wiring that lacks key respiratory enzymes present in mitochondria. Many bacterial enzymes share the common core architecture with the more complex eukaryotic counterparts, but alternative variants and modular adaptations enable the bacterial enzymes to use a much broader set of chemistries. Similar to eukaryotes, some bacteria can also organise their respiratory chain enzymes into higher order supercomplexes, which are 'glued' together by cardiolipin and modularly adapted subunits. Although the exact biological role of such bacterial respirasomes remains unclear, their unique architecture in pathogenic bacteria may provide future possibilities for drug design and open up new ways for treatment of infectious disease, particularly upon emergence of resistance against commonly used antibiotics. Individual members of the bacterial oxidoreductases discussed here, or engineered versions therefore, may also be used in a wide variety of other practical applications, ranging from environmental protection to the sustainable production of fuels for energy supply, thus providing possible solutions both for the pharmaceutical and the energy industry. From a fundamental scientific perspective, future research in the field is strongly focused on integration of structural and mechanistic studies to elucidate fundamental biochemical principles, but it can also provide a pre-requisite for understanding the function of a minimal cell and the molecular origins of life.

References

1. Mitchell, P. Coupling of phosphorylation to electron and hydrogen transfer by a chemi-osmotic type of mechanism. *Nature* **191**, 144–148 (1961).
The basis of modern bioenergetics.
2. Borisov, V. B., Murali, R., Verkhovskaya, M. L., Bloch, D. A., Han, H., Gennis, R. B. & Verkhovsky, M. I. Aerobic respiratory chain of *Escherichia coli* is not allowed to work in fully uncoupled mode. *Proc. Natl. Acad. Sci. USA* **108**, 17320–17324 (2011).
3. Yoshida, M., Muneyuki, E. & Hisabori, T. ATP synthase: A marvellous rotary engine of the cell. *Nat. Rev. Mol. Cell Biol.* **2**, 669–677 (2001).
4. Mulkidjanian, A. Y., Dibrov, P., & Galperin, M. Y. The past and present of sodium energetics: May the sodium-motive force be with you. *Biochim Biophys Acta – Bioenerg.* **1777**, 985–992 (2008).
Concise review of bacterial sodium motif force.
5. Cook, G. M., Greening C., Hards, K. & Berney, M., Energetics of pathogenic bacteria and opportunities for drug development. in *Advances in Microbial Physiology* **65**, 1–62 (2014).
6. Jormakka, M., Byrne, B. & Iwata, S. Protonmotive force generation by a redox loop mechanism. *FEBS Letters*, **545**, 25–30 (2003).
7. Jormakka, M., Törnroth, S., Byrne, B. & Iwata, S. Molecular basis of proton motive force generation: Structure of formate dehydrogenase-N. *Science* **295**, 1863–1868 (2002).
8. Kaila, V. R. I. Long-range proton-coupled electron transfer in biological energy conversion: Towards mechanistic understanding of respiratory complex I. *J. R. Soc. Interface* **15**, 20170916 (2018).
Long-range pumping principles of complex I.
9. Dimroth, P., Jockel, P. & Schmid, M. Coupling mechanism of the oxaloacetate decarboxylase Na+ pump. *Biochim. Biophys. Acta – Bioenerg.* **1505**, 1–14 (2001).

10. Padan, E. & Schuldiner, S. Na^+/H^+ antiporters, molecular devices that couple the Na^+ and H^+ circulation in cells. *J. Bioenerg. Biomembr.* **25**, 647–669 (1993).
11. Häse, C. C., Fedorova, N. D., Galperin, M. Y. & Dibrov, P. A. Sodium ion cycle in bacterial pathogens: evidence from cross-genome comparisons. *Microbiol. Mol. Biol. Rev.* **65**, 353–370 (2001).
12. Haines, T. H. Anionic lipid headgroups as a proton-conducting pathway along the surface of membranes: a hypothesis. *Proc. Natl. Acad. Sci. USA* **80**, 160–164 (1983).
13. Lange, C., Nett, J. H., Trumpower, B. L. & Hunte. C. Specific roles of protein–phospholipid interactions in the yeast cytochrome bc1 complex structure. *EMBO J.* **20**, 6591–6600 (2001).
14. Amdursky, N. Lin, Y. Aho, N. & Groenhof. G. Exploring fast proton transfer events associated with lateral proton diffusion on the surface of membranes. *Proc. Natl. Acad. Sci.* **116**, 2443–2451 (2019).
15. Sandén, T. Salomonsson, L., Brzezinski, P. & Widengren, J. Surface-coupled proton exchange of a membrane-bound proton acceptor. *Proc. Natl. Acad. Sci. USA* **107**, 4129–4134 (2010).
16. Wiseman, B. *et al.* Structure of a functional obligate complex III2IV2 respiratory supercomplex from *Mycobacterium smegmatis*. *Nat. Struct. Mol. Biol.* **25**, 1128–1136 (2018). **The molecular structure of a mycobacterial obligate supercomplex.**
17. Gong, H. *et al.* An electron transfer path connects subunits of a mycobacterial respiratory supercomplex. *Science* **362**, eaat8923 (2018) **The molecular structure of a mycobacterial obligate supercomplex.**
18. Sohlenkamp, C. & Geiger, O. Bacterial membrane lipids: diversity in structures and pathways. *FEMS Microbiology Reviews*, **40**, 133–159 (2016).
19. Kaila, V. R. I., Verkhovsky, M. I. & Wikström, M. Proton-coupled electron transfer in cytochrome oxidase. *Chem. Rev.* **110**, 7062–7081 (2010). **A source of the key concepts of aerobic respiration.**
20. Agmon, N. The Grotthuss mechanism. *Chem. Phys. Lett.* **244**, 456–462 (1995).
21. Nagle, J.F. & Morowitz, H. J. Molecular mechanisms for proton transport in membranes. *Proc. Natl. Acad. Sci. USA* **75**, 298–302 (1978).
22. Marcus, R. A. & Sutin, N. Electron transfers in chemistry and biology. *Biochim. Biophys. Acta. – Bioenerg.* **811**, 265–322 (1985).
23. Beratan, D. N., Onuchic, J. N., Winkler, J. R. & Gray, H. B. Electron-tunneling pathways in proteins. *Science* **258**, 1740–1741(1992). **Breakthrough work on biological electron transfer.**
24. Page, C. C., Moser, C. C., Chen, X. & Dutton, P. L. Natural engineering principles of electron tunnelling in biological oxidation–reduction. *Nature* **402**, 47–52 (1999). **Breakthrough work on the general concept of biological electron transfer.**
25. Kaila, V. R. I., Johansson, MP, Sundholm, D. & Wikström, M. Interheme electron tunneling in cytochrome c oxidase. *Proc. Natl. Acad. Sci. U S A.* **107**, 21470–21475 (2010).
26. Blumberger, J. Recent advances in the theory and molecular simulation of biological electron transfer reactions *Chem. Rev.* **115**, 11191–11238 (2015).
27. Hill, T. L. *Free Energy Transduction and Biochemical Cycle Kinetics* (Springer Verlag New York, Inc. 1989).
28. Tran, Q. H. & Unden, G. Changes in the proton potential and the cellular energetics of Escherichia coli during growth by aerobic and anaerobic respiration or by fermentation. *Eur. J. Biochem.* **251**, 538–543 (1998).
29. Walker, J.E. The ATP synthase: the understood, the uncertain and the unknown. *Biochem. Soc. Trans.* **41**, 1–16 (2013).
30. Preiss, L., Langer, J. D., Yildiz, Ö., Eckhardt-Strelau, L., Guillemont, J. E., Koul, A. & Meier, T. (2015) Structure of the mycobacterial ATP synthase fo rotor ring in complex with the anti-TB drug bedaquiline. *Sci. Adv.* **1**, e1500106–e1500109 (2015).
31. Guo, H., Suzuki, T. & Rubinstein J. L. Structure of a bacterial ATP synthase. *eLife* **8**, e43128 (2019). **A recent summary of bacterial ATP synthases.**
32. Schlegel, K., Leone, V., Faraldo-Gómez, J. D. & Müller, V. Promiscuous archaeal ATP synthase concurrently coupled to Na^+ and H^+ translocation. *Proc. Natl. Acad. Sci. USA* **109**, 947–952 (2012).
33. Wikström, M. & Hummer, G. Stoichiometry of proton translocation by respiratory complex I and its mechanistic implications. *Proc. Natl. Acad. Sci. USA*, **109**, 4431–4436 (2012).
34. Hinkle, P. C. P/O ratios of mitochondrial oxidative phosphorylation. *Biochim. Biophys. Acta – Bioenerg.* **1706**, 1–11 (2005).
35. Petersen, J., Förster, K., Turina, P. & Gräber, P. Comparison of the H^+/ATP ratios of the H^+-ATP synthases from yeast and from chloroplast. *Proc Natl Acad Sci USA* **109**, 11150–11155 (2012).
36. Soga N, Kimura, K., Kinosita, K., Yoshida, M. & Suzuki, T. Perfect chemomechanical coupling of F_oF_1-ATP synthase. *Proc. Natl. Acad. Sci. USA* **114**, 4960–4965 (2017).
37. Jones, A. J. Y., Blaza, J. N., Varghese, F. & Hirst, J. Respiratory complex I in *Bos taurus* and *Paracoccus denitrificans* pumps four protons across the membrane for every NADH oxidized. *J. Biol. Chem.* **292**, 4987–4995 (2017).

38. Westerhoff, H. V., Hellingwerf, K. J. & Van Dam, K. Thermodynamic efficiency of microbial growth is low but optimal for maximal growth rate. *Proc. Natl. Acad. Sci. USA.* **80,** 305–309 (1983).
39. England J. L. Statistical physics of self-replication *J. Chem. Phys*. ***139***, 121923 (2013).
40. Crofts, A. R. The cytochrome bc1 complex: function in the context of structure. *Annu. Rev. Physiol.* **66**, 689–733 (2004)
A central review on complex III.
41. Nowicka, B. & Kruk, J. Occurrence, biosynthesis and function of isoprenoid quinones. *Biochim Biophys Acta – Bioenerg.* **1797**, 1587–1605 (2010).
42. Jones, R.W. & Garland, P.B. The function of ubiquinone and menaquinone in the respiratory chain of *Escherichia coli*. Functions of quinones in energy conserving systems. *Ed.* Trumpower, BL (Academic Press, New York, USA), 465–476 (1982).
43. Yankovskaya, V., Horsefield, R., Törnroth, S., Luna-Chavez, C., Miyoshi, H., Leger, C., Byrne, B., Cecchini, G. & Iwata, S. Architecture of succinate dehydrogenase and reactive oxygen species generation. *Science* **299**, 700–704 (2003).
Structure of *E. coli* complex II.
44. Calhoun, M. W., Oden, K. L., Gennis, R. B., de Mattos, M. J. & Neijssel, O. M. Energetic efficiency of Escherichia coli: Effects of mutations in components of the aerobic respiratory chain. *J. Bacteriol.* **175**, 3020–3025 (1993).
45. Hino, T., Matsumoto, Y., Nagano, S., Sugimoto, H., Fukumori, Y., Murata, T., Iwata, S. & Shiro, Y. Structural basis of biological N_2O generation by bacterial nitric oxide reductase. *Science* **330**, 1666–1670 (2010).
The first resolved molecular structure of a bacterial nitric oxidase reductase.
46. Matsumoto, Y., Tosha, T., Pisliakov, A. V., Hino, T., Sugimoto, H., Nagano, S., Sugita, Y. & Shiro, Y. Crystal structure of quinol-dependent nitric oxide reductase from *Geobacillus stearothermophilus. Nat. Struct. Mol. Biol.* **19**, 238–245 (2012).
47. de Gier, J-W. L., Lübben, M., Reijnders, W. N. M., Tipker, C. A., Slotboom, D.-J., van Spanning, R. J. M., Stouthamer A.H. & van der Oost J. The terminal oxidases of *Paracoccus denitrificans*, *Mol Microbiol.* **13**, 183–196 (1994).
48. Puustinen, A., Finel, M., Virkki, M. & Wikström, M. Cytochrome o (bo) is a proton pump in *Paracoccus denitrificans* and *Escherichia coli*. *FEBS Lett*. **249**, 163–167 (1989).
A first account of proton pumping by bacterial oxidases.
49. Verkhovskaya, M. L., Garcìa-Horsman, A., Puustinen, A., Rigaud, J. L., Morgan, J. E., Verkhovsky, M. I. & Wikström, M. Glutamic acid 286 in subunit I of cytochrome bo3 is involved in proton translocation. *Proc. Natl. Acad. Sci. USA* **94**, 10128–10131 (1997).
50. Borisov, V.B., Gennis, R. B., Hemp, J. & Verkhovsky, M. I. The cytochrome *bd* respiratory oxygen reductases. *Biochim. Biophys. Acta* **1807**, 1398–413 (2011).
51. Bekker, M., de Vries, S., Ter Beek, A., Hellingwerf, K. J. & de Mattos, M. J. Respiration of Escherichia coli can be fully uncoupled via the nonelectrogenic terminal cytochrome bd-II oxidase. *J. Bacteriol.* **191**, 5510–5517 (2009).
52. Kerscher, S., Dröse, S., Zickermann, V. & Brandt, U. The three families of respiratory NADH dehydrogenases. *Results and Problems in Cell Differentiation* **45**, 185–222 (2008).
53. Melo, A. M. P., Bandeiras, T. M. & Teixeira, M. New Insights into Type II NAD(P)H:Quinone Oxidoreductases. *Microbiol. Mol. Biol. Rev.* **68**, 603–616 (2004).
54. Bogachev, A., Murtazina, R. A. & Skulachev, V. P. The Na^+/e^- stoichiometry of the Na^+-motive NADH: quinone oxidoreductase in *Vibrio alginolyticus*. *FEBS Letters* **409**, 475–477 (1997)
55. Verkhovsky, M. I. & Bogachev, A. V. Sodium-translocating NADH:quinone oxidoreductase as a redox-driven ion pump. *Biochim. Biophys. Acta – Bioenerg*. **1797**, 738–746 (2010).
56. Hirst, J. Mitochondrial complex I. *Annu. Rev. Biochem*. **82**, 551–575 (2013).
57. Brandt, U. Energy converting NADH: ubiquinone oxidoreductase (complex I). *Annu. Rev. Biochem.* **75**, 69–92 (2006).
58. Sazanov, L. A. A giant molecular proton pump: structure and mechanism of respiratory complex I. *Nat. Rev. Mol. Cell Biol*. **16**, 375–388 (2015).
59. Baradaran, R., Berrisford, J. M., Minhas, G. S. & Sazanov, L. A. Crystal structure of the entire respiratory complex I. *Nature* **494**, 443–448 (2013).
The first complete molecular structure of the bacterial complex I.
60. Ohnishi, T. Iron-sulfur clusters/semiquinones in complex I. *Biochim. Biophys. Acta – Bioenerg*. **1364**, 186–206 (1998).
61. Hunte, C., Zickermann, V. & Brandt, U. Functional modules and structural basis of conformational coupling in mitochondrial complex I. *Science* **329**, 448–451 (2010).
62. Verkhovskaya M. L., Belevich, N., Euro, L. & Wikström, M. Real-time electron transfer in respiratory complex I. *Proc. Natl Acad. Sci. USA* **105**, 3763–3767 (2008).
63. Lambert A. J. & Brand M. D. Superoxide production by NADH:ubiquinone oxidoreductase (complex I) depends on the pH gradient across the mitochondrial inner membrane. *Biochem. J*. **382**, 511–517 (2004).
64. Zickermann, V., Wirth, C., Nasiri, H., Siegmund, K., Schwalbe, H., Hunte, C. & Brandt, U. Mechanistic

583 insight from the crystal structure of mitochondrial complex I. *Science* **347**, 44–49 (2015).
584 65. Brandt, U. Adaptations of an ancient modular machine. *Science* **363**, 230–231 (2019).
585 66. Yu, H. *et al.* Structure of an Ancient Respiratory System. *Cell* **173**, 1636–1649.e16 (2018).
586 **First structure of an archaeal membrane-bound hydrogenase.**
587 67. Olson, J. W. & Maier, R. J. Molecular hydrogen as an energy source for *Helicobacter pylori*. *Science*, **298**, 1788–
588 1790 (2002).
589 68. Schuller, J. M., Saura, P., Thiemann, J., Schuller, S. K., Gamiz-Hernandez, A. P., Kurisu, G., Nowaczyk, M. M.
590 & Kaila, V. R. I. Redox-coupled proton pumping drives carbon concentration in the photosynthetic complex I.
591 *Nat. Comms*. **11**, 494 (2020).
592 **Molecular adaptations enabling cyanobacterial carbon concentration.**
593 69. Schuller, J. M. *et al* Structural adaptations of photosynthetic complex I enable ferredoxin-dependent electron
594 transfer. *Science* **363**, 257–260 (2019).
595 70. Laughlin, T. G., Bayne, A. N., Trempe, J. F., Savage, D. F. & Davies, K. M. Structure of the complex I-like
596 molecule NDH of oxygenic photosynthesis. *Nature* **566**, 411–414 (2019).
597 71. Zhang, C. *et al.* Structural insights into NDH-1 mediated cyclic electron transfer. *Nat. Commun.* **11**, 888 (2020).
598 72. Di Luca, A., Gamiz-Hernandez, A. P. & Kaila, V. R. I. Symmetry-related proton transfer pathways in respiratory
599 complex I. *Proc. Natl. Acad. Sci. USA* **114**, E6314–E6321 (2017).
600 73. Sharma, V., Belevich, G., Gamiz-Hernandez, A. P., Róg, T., Vattulainen, I., Verkhovskaya, M. L., Wikström, M.,
601 Hummer, G. & Kaila, V. R. I. Redox-induced activation of the proton pump in the respiratory complex I. *Proc.*
602 *Natl Acad. Sci. USA* **112,** 11571–11576 (2015).
603 74. Euro, L., Belevich, G., Verkhovsky, M. I., Wikström, M. & Verkhovskaya, M. Conserved lysine residues of the
604 membrane subunit NuoM are involved in energy conversion by the proton-pumping NADH:ubiquinone
605 oxidoreductase (Complex I). *Biochim Biophys Acta.* **1777**, 1166–1172 (2008).
606 75. Sena, F. V. *et al.* Type-II NADH:quinone oxidoreductase from *Staphylococcus aureus* has two distinct binding
607 sites and is rate limited by quinone reduction. *Molecular microbiology* **98**, 272–288 (2015).
608 76. Feng, Y. *et al.* Structural insight into the type-II mitochondrial NADH dehydrogenases. *Nature* **491**, 478–482
609 (2012).
610 77. Iwata, M.*, et al.* The structure of the yeast NADH dehydrogenase (Ndi1) reveals overlapping binding sites for
611 water- and lipid-soluble substrates*. Proc. Natl. Acad. Sci. USA* **109**, 15247–15252 (2012).
612 78. Harbut, M.B. *et al.* Small Molecules Targeting Mycobacterium tuberculosis Type II NADH Dehydrogenase
613 Exhibit Antimycobacterial Activity. *Angew Chem Int Ed* **57**, :3478–3482 (2018).
614 79. Steuber, J., Vohl, G., Casutt, M. S., Vorburger, T., Diederichs, K. & Fritz, G. Structure of the *V. cholerae* Na^+-
615 pumping NADH:quinone oxidoreductase. *Nature* **516**, 62–77 (2014).
616 80. Belevich, N. P., Bertsova, Y. V., Verkhovskaya, M. L., Baykov, A. A. & Bogachev, A. V. Identification of the
617 coupling step in Na(+)-translocating NADH:quinone oxidoreductase from real-time kinetics of electron transfer.
618 *Biochim Biophys Acta.* **1857**, 141–149 (2016).
619 81. Kurisu, G., Zhang, H., Smith, J. L. & Cramer, W. A. Structure of the cytochrome b6f complex of oxygenic
620 photosynthesis: Tuning the cavity. *Science* **302**, 1009–1014 (2003).
621 82. Mitchell, P. Possible molecular mechanisms of the protonmotive function of cytochrome systems. *J. Theor. Biol.*
622 **62**, 327–367 (1976).
623 83. Kao, W. C. & Hunte, C. The molecular evolution of the Qo motif. *Genome Biol. Evol*. **7**, 1894–1910 (2014).
624 84. Sousa, J.S., Calisto, F., Langer, J.D., Mills, D.J., Refojo, P.N., Teixeira, M., Kühlbrandt, W., Vonck, J. & Pereira,
625 M.M. Structural basis for energy transduction by respiratory alternative complex III. *Nat. Commun.* **9**, 1728–1728
626 (2018).
627 85. Majumder, E.L.W, King J.D. & Blankenship, R.E. Alternative Complex III from phototrophic bacteria and its
628 electron acceptor auracyanin. *Biochim. Biophys. Acta. – Bioenerg.* **1827**, 1383–1391 (2013).
629 86. Sun, C., Benlekbir, S., Venkatakrishnan, P., Wang, Y., Hong, S., Hosler, J., Tajkhorshid, E., Rubinstein, J. L. &
630 Gennis, R. B. Structure of the alternative complex III in a supercomplex with cytochrome oxidase. *Nature* **557**,
631 123–126 (2018).
632 **Structure of a bacterial supercomplex.**
633 87. Alvarez-Paggi, D., Hannibal, L., Castro, M.A., Oviedo-Rouco, S., Demicheli, V., Tórtora, V., Tomasina, F., Radi,
634 R. & Murgida, D.H. Multifunctional Cytochrome **c**: Learning New Tricks from an Old Dog. *Chem. Rev*. **117**,
635 13382–13460 (2017).
636 88. Kao, W. C. *et al.* The obligate respiratory supercomplex from Actinobacteria. *Biochim. Biophys. Acta - Bioenerg.*
637 **1857**, 1705–1714 (2016).
638 89. Buschmann, S., Warkentin, E., Xie, H., Langer, J. D., Ermler, U. & Michel, H. The Structure of cbb3 cytochrome
639 oxidase provides insights into proton pumping. *Science* **329**, 327–330 (2010).
640 90. Lyons, J.A., Aragao, D., Slattery, O., Pisliakov, A.V., Soulimane, T. & Caffrey, M. Structural Insights Into
641 Electron Transfer in Caa3-Type Cytochrome Oxidases. *Nature* **487**, 514–518 (2012).
642 91. Abramson, J., *et al.* The structure of the ubiquinol oxidase from Escherichia coli and its ubiquinone binding site.
643 *Nat. Struct. Biol.* **7**, 910–917 (2000).

92. Xu, J. *et al.* Structure of the cytochrome aa3-600 heme-copper menaquinol oxidase bound to inhibitor HQNO shows TM0 is part of the quinol binding site. *Proc. Natl. Acad. Sci. USA.* **117**, 872–876 (2020).
93. Wikström, M., Sharma, V., Kaila, V. R. I., Hosler, J. P & Hummer, G. New perspectives on proton pumping in cellular respiration. *Chem. Rev*. **115**, 2196–2221 (2015).
94. Wikström, M. K. F. Proton pump coupled to cytochrome c oxidase in mitochondria. *Nature* **266**, 271–273 (1977). **The discovery of cytochrome oxidase as a proton pump.**
95. Pereira, M. M., Santana, M. & Teixeira, M. A novel scenario for the evolution of haem-copper oxygen reductases. *Biochim. Biophys. Acta - Bioenerg.* **1505**, 185–208 (2001).
96. Chang, H. Y., Hemp, J., Chen, Y., Fee, J. A. & Gennis, R. B., The cytochrome ba3 oxygen reductase from *Thermus thermophilus* uses a single input channel for proton delivery to the active site and for proton pumping. *Proc. Natl. Acad. Sci. USA* **106**, 16169–16173 (2009).
97. Rauhamäki, V., Bloch, D. A. & Wikström, M. Mechanistic stoichiometry of proton translocation by cytochrome cbb3. *Proc. Natl. Acad. Sci. USA*. **109**, 7286–7291 (2012).
98. Hendriks, J. H., Jasaitis, A., Saraste, M. & Verkhovsky, M. I. Proton and electron pathways in the bacterial nitric oxide reductase. *Biochemistry* **41**, 2331–2340 (2002).
99. Blomberg, M. R. A. & Ädelroth, P. Mechanisms for enzymatic reduction of nitric oxide to nitrous oxide - A comparison between nitric oxide reductase and cytochrome c oxidase. *Biochim. Biophys. Acta - Bioenerg*. **1859**, 1223–1234 (2018).
100. Gonska, N. *et al.* Characterization of the quinol-dependent nitric oxide reductase from the pathogen Neisseria meningitidis, an electrogenic enzyme. *Sci. Rep.* **8**, 3637 (2018).
101. Wikström, M., Krab, K. & Sharma, V. Oxygen Activation and Energy Conservation by Cytochrome c Oxidase. *Chem. Rev.* **118**, 2469–2490 (2018).
102. Belevich, I., Verkhovsky, M. I. & Wikström, M. Proton-coupled electron transfer drives the proton pump of cytochrome *c* oxidase. *Nature* **440**, 829–832 (2006).
103. Wikström, M., Verkhovsky, M. I. & Hummer, G. Water-gated mechanism of proton translocation by cytochrome c oxidase. *Biochim. Biophys. Acta. – Bioenerg*. **1604**, 61–65 (2003).
104. Supekar, S. & Kaila, V. R. I. Dewetting transitions coupled to K-channel activation in cytochrome *c* oxidase. *Chem. Sci.* **9**, 6703–6710 (2018).
105. Saura, P., Frey, D.M., Gamiz-Hernandez, A.P. & Kaila, V.R.I. Electric field modulated redox-driven protonation and hydration energetics in energy converting enzymes. *Chem Comm* **55**, 6078–6081 (2019).
106. Kaila, V.R.I., Verkhovsky, M.I., Hummer, G. & Wikström, M. Glutamic acid 242 is a valve in the proton pump of cytochrome c oxidase. *Proc Natl Acad Sci USA*. **105**, 6255–6259 (2008)
107. Rauhamäki, V., Bloch, D. A., Verkhovsky, M. I. & Wikström, M. Active site of cytochrome cbb3. *J. Biol. Chem*. **284**, 11301–11308 (2009).
108. Giuffrè A, Stubauer, G., Sarti, P., Brunori, M., Zumft, W. G., Buse, G. & Soulimane T. The heme-copper oxidases of Thermus thermophilus catalyze the reduction of nitric oxide: Evolutionary implications. *Proc. Natl. Acad. Sci. U. S. A.* **96**, 14718–14723 (1999)
109. Huang, Y., Reimann, J., Lepp, H., Drici, N. & Ädelroth, P. Vectorial proton transfer coupled to reduction of O2 and NO by a heme-copper oxidase. *Proc Natl Acad Sci USA*. **105**, 20257–20262 (2008).
110. Puustinen, A. & Wikström, M. The heme groups of cytochrome o from *Escherichia coli*. *Proc. Natl. Acad. Sci. USA*. **88**, 6122–6126 (1991).
111. Safarian, S., *et al.* Active site rearrangement and structural divergence in prokaryotic respiratory oxidases. *Science* **366**, 100–104 (2019).
112. Safarian, S., Rajendran, C., Müller, H., Preu, J., Langer, J. D., Ovchinnikov, S., Hirose, T., Kusumoto, T., Sakamoto, J. & Michel H. Structure of a bd oxidase indicates similar mechanisms for membrane-integrated oxygen reductases. *Science* **352**, 583–586 (2016). **The molecular structure of the bacterial bd oxidase.**
113. Schägger, H. Respiratory chain supercomplexes of mitochondria and bacteria. *Biochim Biophys Acta.* **1555**, 154–159 (2002)
114. Letts, J. A., Fiedorczuk, K., Degliesposti, G., Skehel, M. & Sazanov, L. A. Structures of Respiratory Supercomplex I+III2 Reveal Functional and Conformational Crosstalk. *Mol. Cell* **75**, 1131–1146.e6 (2019).
115. Davies, K. M., Blum, T. B. & Kühlbrandt, W. Conserved in situ arrangement of complex I and III(2) in mitochondrial respiratory chain supercomplexes of mammals, yeast, and plants. *Proc. Natl. Acad. Sci. USA* **115**, 3024–3029 (2018).
116. Stuchebrukhov, A., Schäfer, J., Berg, J. & Brzezinski, P. Kinetic advantage of forming respiratory supercomplexes. *Biochim Biophys Acta Bioenerg*. **1861**, 148193 (2020)
117. Bianchi, C., Genova, M. L., Parenti Castelli, G. & Lenaz, G. The mitochondrial respiratory chain is partially organized in a supercomplex assembly: kinetic evidence using flux control analysis. *J. Biol. Chem.* **279**, 36562–36569 (2004).
118. Fedor, J. G. & Hirst, J. Mitochondrial Supercomplexes Do Not Enhance Catalysis by Quinone Channeling. *Cell Metab.* **28**, 525–531.e4 (2018).

119. Blaza, J. N., Serreli, R. Jones, A. J. Y., Mohammed, K. & Hirst, J. Kinetic evidence against partitioning of the ubiquinone pool and the catalytic relevance of respiratory-chain supercomplexes. *Proc. Natl. Acad. Sci. USA* **111** 15735–15740 (2014).
120. Efremov, R.G. & Sazanov, L.A. Structure of the membrane domain of respiratory complex I. *Nature* **476**, 414–420 (2011).
121. Heikal, A. *et al.* Structure of the bacterial type II NADH dehydrogenase: A monotopic membrane protein with an essential role in energy generation. *Mol. Microbiol.* **91**, 950–964 (2014).
122. Sousa, F. M. *et al.* The key role of glutamate 172 in the mechanism of type II NADH:quinone oxidoreductase of Staphylococcus aureus. *Biochim. Biophys. Acta - Bioenerg.* **1858**, 823–832 (2017).
123. Kleinschroth, T., Castellani, M., Trinh, C. H., Morgner, N., Brutschy, B., Ludwig, B. & Hunte, C. X-ray structure of the dimeric cytochrome bc(1) complex from the soil bacterium *Paracoccus denitrificans* at 2.7-Å resolution. *Biochim. Biophys. Acta – Bionenerg*. **1807**,1606–1615 (2011).
124. Koepke, J., Olkhova, E., Angerer, H., Müller, H., Peng, G. & Michel, H. High resolution crystal structure of *Paracoccus denitrificans* cytochrome c oxidase: New insights into the active site and the proton transfer pathways. *Biochim. Biophys. Acta – Bioenerg.* **1787**, 635–645 (2009).
125. Tiefenbrunn, T., Liu, W., Chen, Y., Katritch, V., Stout, C. D., Fee, J. A. & Cherezov, V., High resolution structure of the ba3 cytochrome c oxidase from Thermus thermophilusin a lipidic environment. *PLoS One*,.**6**, e22348 (2011).
126. Thesseling, A., Rasmussen, T., Burschel, S., Wohlwend, D., Kagi, J., Muller, R., Bottcher, B. & Friedrich, T. Homologous bd oxidases share the same architecture but differ in mechanism. *Nat. Commun.* **10**, 5138–5138 (2019).
127. Cunningham, L., M. Pitt, M. & Williams H. D. The *cioAB* genes from *Pseudomonas aeruginosa* code for a novel cyanide-insensitive terminal oxidase related to the cytochrome *bd* quinol oxidases. *Mol. Microbiol.* **24**, 579–591 (1997).

Acknowledgment

VRIK acknowledges insightful discussion with Peter Brzezinski, as well as all members of the Kaila Lab. This work was supported by the European Research Council (ERC) and the Knut and Alice Wallenberg (KAW) Foundation (VRIK). MW acknowledges a grant from the Magnus Ehrnrooth Foundation. This work was also supported by the Swedish National Infrastructure for Computing (SNIC 2020/1-38) at PDC Centre, partially funded by the Swedish Research Council through grant agreement no. 2016-07213.

Table 1. Examples of resolved structures of bacterial respiratory chain enzymes.

Protein	Organism	Function (q^+/e^-)	PDB ID (resolution)	References
Type I & II NADH:Q oxidoreductases				
Complex I/NDH-1	*E. coli*	NADH → Q 2 H^+/e^-	3RKO, 3.0 Å	[120]
	T. thermophilus	NADH → MQ 2 H^+/e^-	4HEA, 3.3 Å	[59]
NDH-2	*C. thermarum*	0 H^+/e^-	4NWZ, 2.5 Å	[121]
	S. aureus	0 H^+/e^-	5NA4, 2.6 Å	[122]
NDH-1L NDH-1MS	*T. elognatus*	Fd → PQ 2 H^+/e^- *	6TJV, 6HUM, 6NBY, 6KHJ, 3.0-3.3 Å	[68, 69, 70, 71]
Mbh	*P. furiosus* (archeon)	Fd → PQ 1 H^+/e^-, Na^+/H^+ *	6CWF, 3.7 Å	[66]
Nqr	*V. cholerae*	NADH → Q 1 Na^+/e^-*	4P6V, 3.5 Å	[79]
Complex III				
Complex III (bc_1)	*P. denitrificans*	QH_2 → *cyt c* 2 H^+/e^-	2YIU, 2.7 Å	[123]
Alternative complex III	*R. marinus*	QH_2→ O_2	6F0K, 3.9 Å	[86]
Terminal heme-copper oxidases				
aa_3	*P. denitrificans*	*cyt c* → O_2 2 H^+ / e^-	3HB3, 2.3 Å	[124]
aa3-MQ oxidase	*B. subtilis*	MQH_2→O_2	6KOE, 3.75 Å	[92]
bo_3	*E. coli*	QH_2→O_2 2 H^+/e^-	1FFT, 3.5 Å	[91]
ba_3	*T. thermophilus*	*cyt c* → O_2	3S8F, 1.8 Å	[125]
cbb_3	*P. stutzeri*	1 H^+/e^-	3MK7, 3.2 Å	[89]
cNOR	*P. aeruginosa*	2NO→ N_2O	3O0R, 2.7 Å	[45]
qNOR	*G. stearothermophilus*	2NO→ N_2O 1 H^+/e^- *	3AYF, 2.5 Å	[46]
bd-I oxidase	*E. coli*	QH_2→ O_2 1 H^+/e^-	6RKO, 2.7 Å; 6RX4, 3.3 Å	[111, 126]
bd-II oxidase	*G. thermo-denitrificans*	QH_2→ O_2 0 [45] or 1 H^+/e^- [2]	5DOQ, 3.1 Å	[112]
Bacterial supercomplexes				
III_2-IV_2	*M. smegmatis*	MQH_2→ O_2	6HWH, 3.3 Å; 6ADQ, 3.5 Å	[16, 17]
ACIII-IV	*F. johnsoniae*	QH_2→ O_2	6BTM, 3.4 Å	[86]

* no proton pumping measurements available

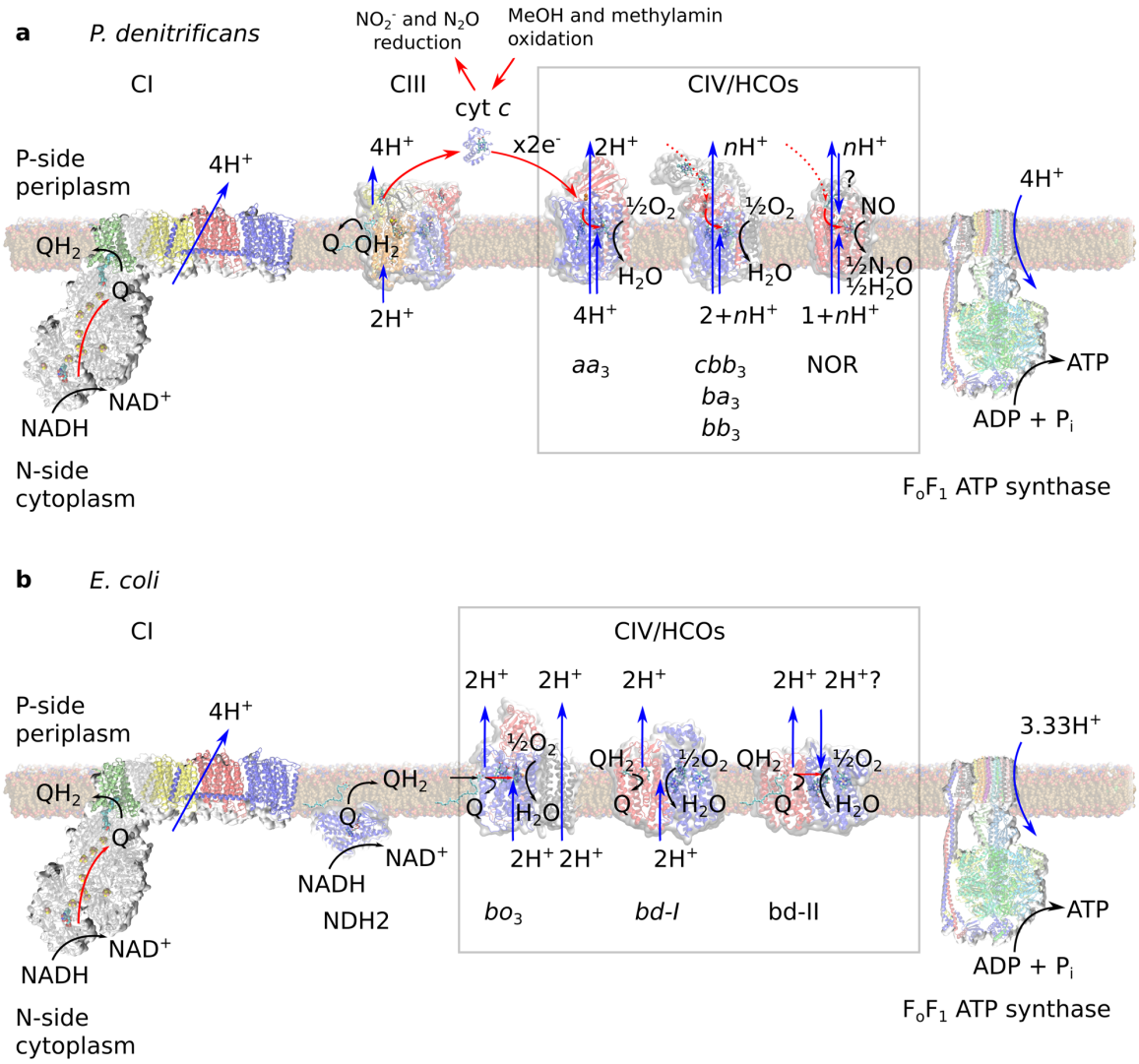

Figure 1. Examples of bacterial respiratory chains. Schematic representation of PMF-generating aerobic bacterial respiratory chains from **a**, *P. denitrificans* and **b,** *E. coli.* The reported proton pumping is given for two electron reduction steps. Complex II (succinate dehydrogenase) is not shown as the focus here is on PMF-generating respiratory chains.

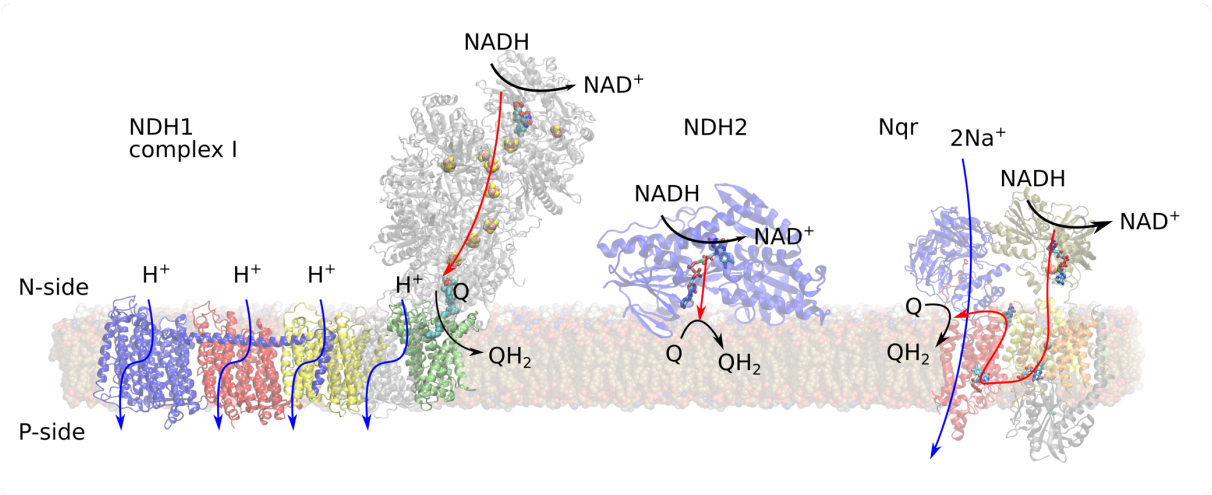

Figure 2. **Structure and function of initial electron acceptors in bacterial respiratory chains.** The figure shows Type I and Type-II NADH oxidoreductases, with NDH1 (complex I, PDB ID: 4HEA, *left*) and NDH2 (PDBI ID: 4NWZ, *middle*), and the Na^+-pumping Nqr (PDB ID: 4P6V, *right*).

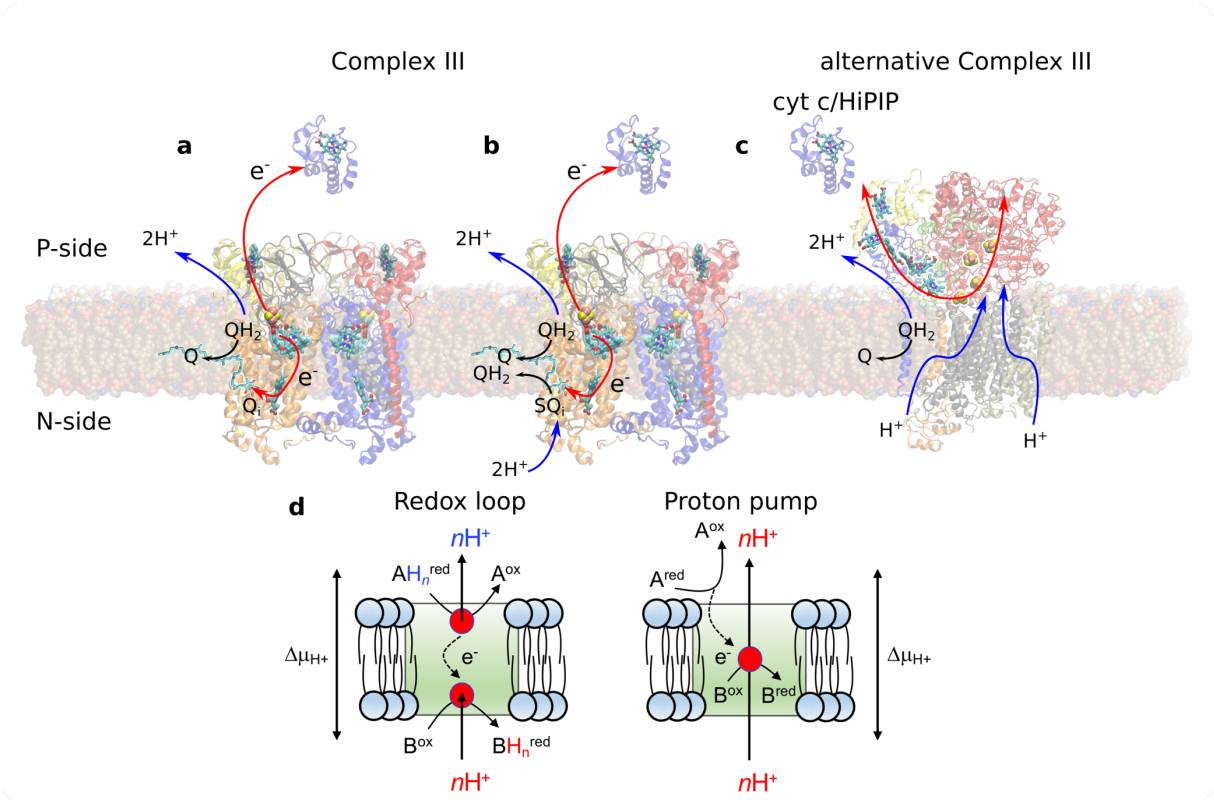

Figure 3. **The bacterial complex III and its Q-cycle mechanism. a**, Oxidation of quinol in the Q_o site of complex III (PDB ID: 2YIU), drives proton release to the P-side and reduction of *cyt c* and a second quinone at the Qi site by a bifurcated electron transfer process. **b**, Oxidation of a second quinol at the Q_o site, leads to a similar process as in **a**, and complete reduction of the semiquinone (SQ) at the Q_i site and uptake of protons from the N-side. **c**, the structure of the alternative complex III from *Rhodobacter marinus* (PDB ID: 6F0K). **d**, Schematic representation of a redox-loop (left) and proton pump (right). In redox loops, for example, complex III, the protons are released on respective sides of the membrane, while the electrical charge is translocated as transmembrane electron transfer. The protons are transferred electroneutrally across the membrane as hydrogen atoms[82]. In redox-driven proton pumps, such as cytochrome *c* oxidase or complex I, the protons are transferred across the membrane dielectric, driven by the redox reaction.

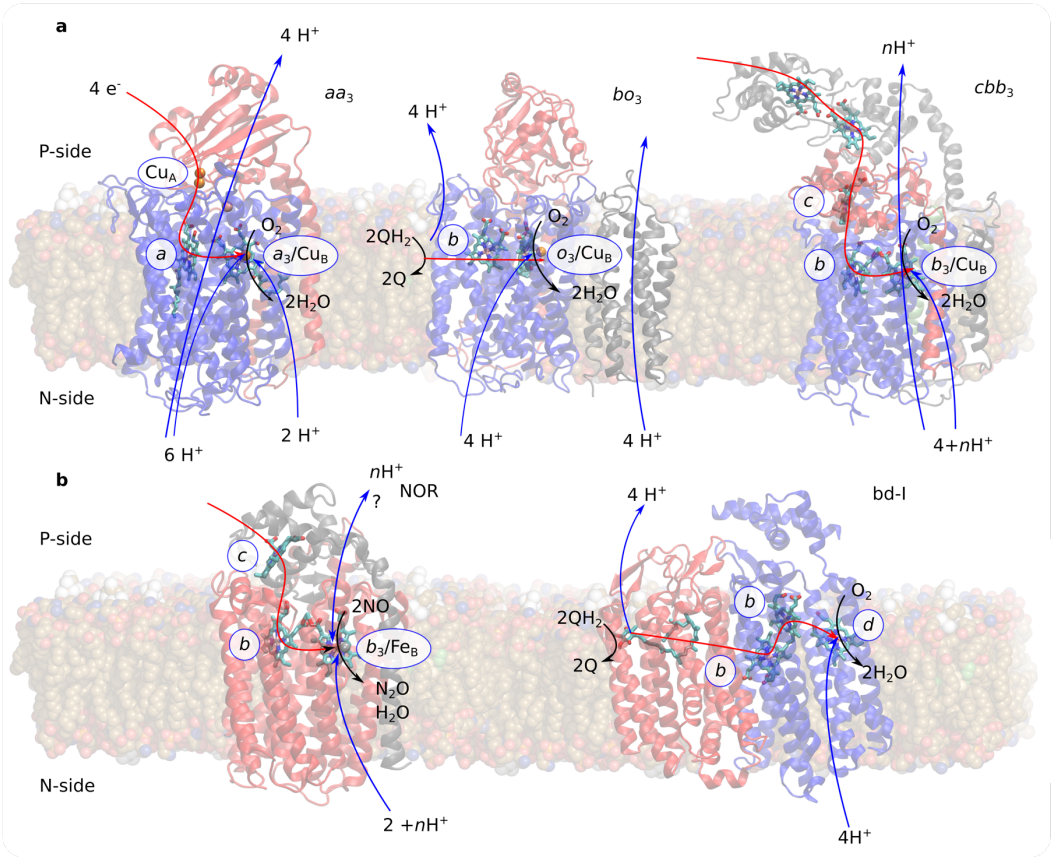

Figure 4. Bacterial terminal respiratory oxidases. a, The figure shows terminal HCO-oxidases (*aa*$_3$ (PDB ID: 3HB3), *bo*$_3$ (PDB ID: 1FFT), and *cbb*$_3$ (PDB ID:3MK7)), **b**, cNOR (PDB ID: 3O0R) and *bd*-I oxidase (PDB ID: 6RKO). The figure shows the complete four-electron reduction that complete one catalytic cycle.

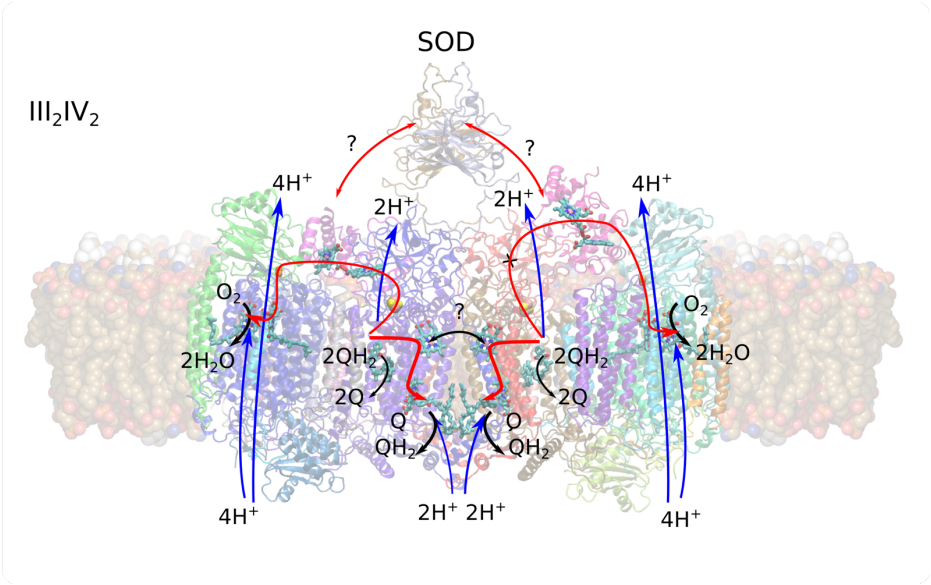

Figure 5. **Bacterial respiratory supercomplexes.** The bacterial III_2IV_2 supercomplex from *M. smegmatis* (model based on PDB ID: 6HWH) and its possible charge transfer pathways is shown. In the resolved structure, one of the mobile *cyt c* domains is in a conformation expected to prevent electron transfer to the complex IV unit on the right side[16, 17]. The SOD domain is not well-resolved in the cryoEM maps, but here modelled based on atomistic simulations.

[G] Glossary terms

Zwitterionic lipids: lipid molecules that carry both negative and positive electric point charges

Desolvation (Born) free energy: the electrostatic component of free energy arising from ion solvation

Grotthuss-type: an excess proton that diffuses within a hydrogen-bonded network of residues via the concerted formation and breaking of covalent bonds between donor and acceptor pairs, followed by re-orientation of the hydrogen-bonded network. Named after C.J.T. von Grotthuss who proposed the mechanism in 1806.

Rieske iron-sulphur protein: the Rieske iron-sulphur protein is the Fe_2S_2 centre of complex III and is named after its discoverer, the late John S. Rieske

Mitchellian redox-loop mechanism: the 'redox-loop' is the original proton translocation principle in Peter Mitchell's chemiosmotic theory, which involves direct electron transfer from the P-side to the N-side and coupled proton release and uptake reactions at respective sides of the membrane